Binding of a Gating Modifier Toxin Induces Intersubunit Cooperativity Early in the Shaker K Channel's Activation Pathway

Jon T. Sack and Richard W. Aldrich

Howard Hughes Medical Institute and Department of Molecular and Cellular Physiology, Stanford University School of Medicine, Stanford, CA 94305

Potassium currents from voltage-gated Shaker K channels activate with a sigmoid rise. The degree of sigmoidicity in channel opening kinetics confirms that each subunit of the homotetrameric Shaker channel undergoes more than one conformational change before the channel opens. We have examined effects of two externally applied gating modifiers that reduce the sigmoidicity of channel opening. A toxin from gastropod mucus, 6-bromo-2-mercaptotryptamine (BrMT), and divalent zinc are both found to slow the same conformational changes early in Shaker's activation pathway. Sigmoidicity measurements suggest that zinc slows a conformational change independently in each channel subunit. Analysis of activation in BrMT reveals cooperativity among subunits during these same early steps. A lack of competition with either agitoxin or tetraethylammonium indicates that BrMT binds channel subunits outside of the external pore region in an allosterically cooperative fashion. Simulations including negatively cooperative BrMT binding account for its ability to induce gating cooperativity during activation. We conclude that cooperativity among K channel subunits can be greatly altered by experimental conditions.

The Journal of General Physiology

INTRODUCTION

The ShakerBΔ K channel (ShBΔ) is a homotetrameric protein complex (MacKinnon, 1991). In response to a voltage stimulus, each of the four identical channel subunits undergo multiple activating conformational changes followed by opening of the central channel pore (Zagotta et al., 1994a,b; Baker et al., 1998; Schoppa and Sigworth, 1998c). In this paper we investigate how conformational change in a subunit influences conformational change in other subunits.

When ShBΔ channels activate, some steps are cooperative among subunits and others appear to be independent. Transitions earlier in ShBΔ's activation path do not appear to interact among subunits and may occur completely independently of each other. Definitively cooperative processes do not occur until later in the activation path. The final opening step of ShBΔ is known to be highly cooperative: all four subunits activate in a nearly concerted fashion (Schoppa and Sigworth, 1998a,b,c; Smith-Maxwell et al., 1998a,b; Pathak et al., 2005). At what point in the activation path the switch to highly cooperative dynamics occurs is not clear. Furthermore, because of the relative difficulty in studying early gating steps, the possibility that these steps are cooperative has not been excluded.

Well constrained kinetic models of ShBΔ's activation path find that activation dynamics can be well described without invoking early cooperativity (Zagotta et al., 1994a). In most modeling, complete independence is invoked among early steps because modeling intersubunit cooperativity requires additional free parameters. However, at the cost of introducing extra free parameters, including a modicum of cooperativity improves model fits to the experimental data (Zagotta et al., 1994a; Schoppa and Sigworth, 1998c). Aside from this ability of added cooperative parameters to moderately improve fits to experimental results, there is no evidence that early gating steps of ShBΔ channels are cooperative amongst subunits.

A few studies have looked for intersubunit cooperativity amongst early steps but failed to find it. One creative study found that immobilizing a voltage sensor in one ShBΔ subunit does not immobilize much, if any, of the charge movement in other subunits (Horn et al., 2000). This indicates that the majority of gating charge movement is not highly cooperative among subunits, but leaves open the possibility for some cooperative interaction. Another original experimental approach has shown that voltage-dependent fluorescence changes from dye-labeled ShBΔ subunits can be altered by mutations in other subunits (Mannuzzu and Isacoff, 2000; Pathak et al., 2005). This finding was interpreted to conclude that later gating steps influence other subunits in a cooperative fashion, in agreement with previous conclusions that the highly cooperative final opening transition accounted for the cooperative effects of other subunits. Again, early activation steps appeared independent among subunits in these studies. Taken

Correspondence to Richard W. Aldrich: raldrich@mail.utexas.edu

Abbreviation used in this paper: BrMT, 6-bromo-2-mercaptotryptamine.

together, these studies found little evidence for cooperativity among early steps in the ShBΔ activation pathway, although none of them can definitively conclude that these steps are independent between subunits.

Here we investigate ShBΔ activation by a different means. We use gating modifier ligands to the slow early activation steps in ShBΔ channels. When slowed, these steps become rate limiting for channel activation. When the early steps are rate limiting, they alone determine the time course of I_K activation, and their kinetics and cooperative behavior can be studied in greater detail.

The earliest activation steps of the ShBΔ channel are slowed by a toxin from a marine gastropod's defensive mucus, a disulfide-linked dimer of BrMT (6-bromo-2-mercaptotryptamine) (Kelley et al., 2003; Sack et al., 2004). This toxin stabilizes resting voltage sensors and prevents them from activating. Kinetically, BrMT induces a graded slowing of channel activation. As the concentration of BrMT in solution is increased, channels activate progressively slower. The slowing of I_K activation is accompanied by a reduction in peak I_K, due to BrMT stabilizing an inactivated or unavailable state. The BrMT-induced inactivation appears to occur by a mechanism distinct from the action of BrMT on activation and is ignored intentionally throughout this paper. The channels that do open when exposed to BrMT appear to activate as one homogenous population, where each channel is slowed to an equal degree in a given concentration of toxin. This is evidenced by the ability of a single exponential to fit the latter half of BrMT-slowed K current rise after a voltage step. The time constant of activation is used to quantitate the degree by which BrMT slows ShBΔ activation. The dose–response behavior of BrMT suggests that the toxin slows voltage sensor activation by binding to resting subunits in a rapid manner, such that voltage sensors can be considered to be at an equilibrium with the toxin. When toxin is bound to channels, they cannot activate and channel activation is slowed in proportion to the probability that toxin is bound to channel subunits. Thus, strong negative allosteric coupling between toxin binding and voltage sensor activation slows channel opening.

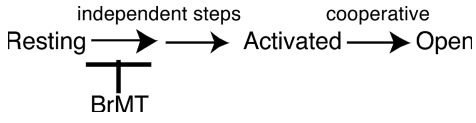

(SCHEME 1)

This scheme summarizes what has been previously determined about the BrMT's effect on ShBΔ's activation path. Early, presumably independent activation steps are slowed but not the highly cooperative final opening transitions.

In this study we apply more extensive kinetic analyses to the waveform of ShBΔ potassium current rise (I_K) in BrMT. Surprisingly, we find that the kinetics of I_K rise are indicative of a high degree of intersubunit cooperativity among the early activation steps. As these early steps are thought to be independent among subunits, we investigate this cooperative behavior more extensively. This leads us to question if the cooperativity observed in BrMT is evidence of intrinsically cooperative activation, or if BrMT itself imparts cooperative behavior on the early steps. To determine whether the cooperativity in BrMT is due to intrinsic channel gating or induced by BrMT, the effects of BrMT were examined with another gating modifier that slows activation, divalent zinc. We conclude that BrMT induces cooperativity early in ShBΔ's activation path by binding cooperatively to subunits. A model of ShBΔ activation that incorporates independent early gating and negative cooperativity in BrMT binding accounts for the changes in gating cooperativity seen in BrMT.

MATERIALS AND METHODS

Channel Expression and Electrophysiology

Xenopus laevis oocytes were injected with ShBΔ RNA as described previously (Sack et al., 2004). The *Drosophila* ShakerBΔ6-46 (ShBΔ) construct had N-terminal residues 6–46 deleted to eliminate fast, N-type inactivation (Hoshi et al., 1990), and had C-type inactivation minimized by the T449Y mutation (Lopez-Barneo et al., 1993). The T449Y mutation had no effect on the degree of slowing or sigmoidicity in BrMT (unpublished observations), but reduced the accumulation of inactivated channels in BrMT (Sack et al., 2004).

Excised oocyte patch recordings were made at 22°C in the outside-out configuration using an Axopatch 200A amplifier. Records were filtered at 10 kHz and digitized at 50 samples/ms. P/−n leak subtraction was used. The holding and leak holding potential was −80 mV. All activating steps were preceded by a 60-ms pulse to −100 mV. Pipette tip resistances were <3 MΩ.

Solutions

BrMT was purified from hypobranchial glands of *Calliostoma canaliculatum* as described previously (Kelley et al., 2003). All concentrations of BrMT cited refer to the active dimeric form. BrMT was diluted from an aqueous stock solution as in Sack et al. (2004).

The internal solution contained (in mM): 50 KF, 60 KCl, 30 KOH, 10 EGTA, 20 HEPES (pH 7.2 with HCl). To prevent internal effects of BrMT, 2 mM tris-carboxyethylphosphine was added to monomerize BrMT should it reach the internal solution (see Sack et al., 2004). Solution pH was then returned to 7.2 with *N*-methyl-D-glucamine and frozen at −20°C until use.

The standard external solution for I_K recordings contained (in mM): 115 NaCl, 10 KCl, 2 $MgCl_2$, 2 $CaCl_2$, 20 HEPES (pH 7.2 with HCl). For TEA experiments, 1 mM tetraethylammonium chloride was added to this solution. Agitoxin-2 (Garcia et al., 1994) from Sigma-Aldrich was suspended in this external solution and kept frozen at −20°C until use. BSA was not added to toxin-containing solutions. While albumen may prevent absorption of toxin to tubing and containers, albumen functionally inactivates BrMT, likely by binding it.

For experiments involving zinc, solution composition was altered. Millimolar concentrations of zinc are difficult to keep in solution at neutral pH, due to the precipitation of zinc hydroxide (for a detailed discussion of zinc solubility see Cherny and DeCoursey, 1999). To ensure zinc solubility at concentrations up

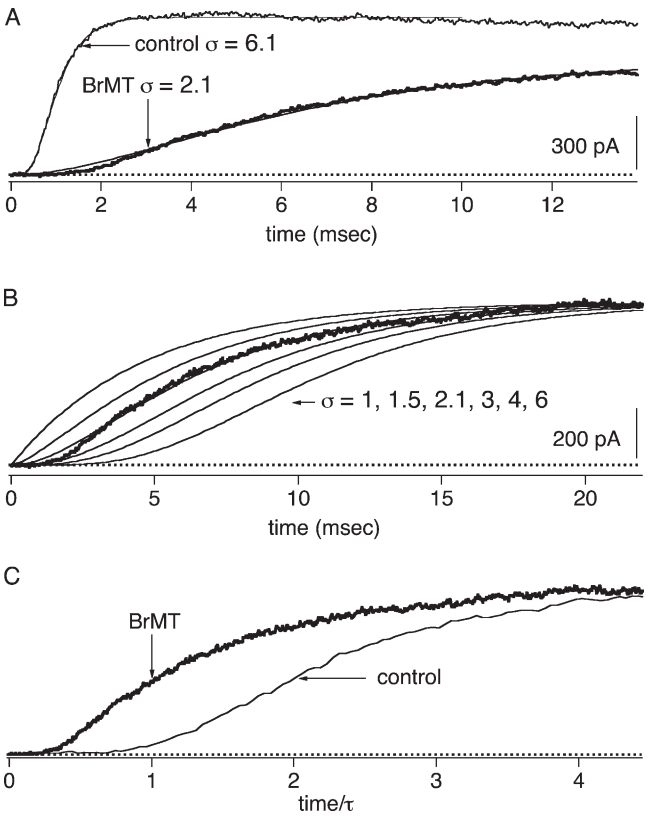

Figure 1. Sigmoidicity of ShakerBΔ activation is reduced by BrMT. (A) Activation of ShBΔ channels at +40 mV in an outside-out patch in the absence (control condition, thin trace) or presence (thick trace) of 5 μM BrMT. Overlaid on the data are fits of Eq. 1 with the indicated σ values. (B) BrMT I_K and the fit of Eq. 1 (same as A) are replotted, and σ from the fit equation was altered to the indicated values. (C) Traces from A scaled in time to such that the time constant of I_K rise from Eq. 1 is the same for both traces. After this scaling procedure, the delay before I_K rise is shorter in BrMT than control.

to 20 mM, different external solutions were made more acidic, pH 6.8. These solutions contained (in mM) 35 NaCl, 90 KCl, 2 $CaCl_2$, 20 HEPES (HCl), with 20 XCl_2 where X could be either magnesium or zinc. Zinc replaced magnesium in an isomolar fashion to keep a constant divalent ion concentration and minimize changes in junction potential and surface charge induced by zinc.

External solutions were applied to outside-out patches in a continuous stream using a delivery manifold with a 100-μm diameter port (DAD-12, ALA Scientific Instruments) and a back pressure of 150–300 mm Hg.

Analysis and Graphing

Analysis and graphing were performed with IgorPro software (Wavemetrics), which performs nonlinear least-squares fits using a Levenberg-Marquardt algorithm. Experimental traces shown were digitally smoothed with a 2-kHz Gaussian filter for presentation. To measure sigmoidicity, data were fit with Eq. 1 from the time of origin until I_K rise was at least 95% complete. The time origin of I_K is the start of the activating voltage pulse after accounting for filter delay. Simulations were performed with procedures in Igor Pro provided by F. Horrigan (Horrigan et al., 1999). Simulated I_K was fit by Eq. 1 until the point where I_K was 99% of maximum. All statistics noted are mean ± SEM.

RESULTS

BrMT Reduces Sigmoidicity of Activation Kinetics

The degree of sigmoidicity in the I_K waveform provides a measure of the minimum number of activation steps that must occur before a K channel opens (see Fig. 1). The degree of sigmoidicity in I_K rise was first quantitated in delayed rectifier K currents from the squid giant axon (Hodgkin and Huxley, 1952). They fit I_K rise with the power of an exponential function to determine underlying rate constants associated with K channel activation. In such studies, sigmoidicity had been used to estimate the number of independent particles or subunits that activate before channel opening. Now, with a cloned K channel known to have four identical subunits, we use sigmoidicity analysis differently, not to count subunits, but to study the cooperative nature of interactions between subunits.

Sigmoidicity analysis routines nicely fit I_K from squid as well as ShBΔ channels (Zagotta et al., 1994b). In this paper we fit the sigmoid waveform of ShBΔ I_K rise using the function

$$I_K = A(1 - e^{-t/\tau})^{\sigma}. \quad (1)$$

Eq. 1 yields a curve that originates at $I_K = 0$ when t (time) = 0 and asymptotically approaches its maximum amplitude, A, with a time course determined by time constant τ and sigmoidicity σ. When σ = 1, Eq. 1 describes a monoexponential rise, as would be expected from an activation process involving one activation transition. As σ increases, the delay before I_K rise increases and I_K becomes sigmoid in shape (Fig. 1 B). In a model where channel opening is preceded by a number of independent and identical activation transitions, the value of σ is the number of transitions required to produce such a sigmoidicity. For example, a homotetrameric K channel with each subunit undergoing one independent activation step before channel opening would have an I_K sigmoidicity of σ = 4. No matter how fast or slow the channel opens, if all four subunits independently activate at the same rate, σ can never be less than 4. Thus, sigmoidicity analysis determines the minimum number of steps that occur before channel opening.

In a real Shaker K channel, many more activating transitions occur than the minimum determined by sigmoidicity analysis. ShBΔ activation has a sigmoidicity of σ ∼ 6 (Zagotta et al., 1994b), but detailed mechanistic studies have concluded that Shaker channels must traverse a minimum of 9 (Smith-Maxwell et al., 1998b) or even 14 (Schoppa and Sigworth, 1998c) steps along the activation pathway. The lower sigmoidicity occurs because the slower conformational transitions disproportionately impact the I_K waveform. Fast conformational changes can be kinetically insignificant or "silent" in sigmoidicity analysis if the fast steps do not limit the

rate of channel opening. The existence of additional fast activation steps does cause a fit discrepancy at the foot of I_K rise; note that Eq. 1 initially rises slightly above experimental I_K . We find that only when a step occurs at a rate within an order of magnitude of the slowest step, does it contribute significantly to the sigmoidicity of activation.

ShBΔ sigmoidicity decreases from $\sigma \sim 6$ to $\sigma \sim 2$ when BrMT is applied to the extracellular side of the patch (Fig. 1 A). The fact that BrMT reduces sigmoidicity may not be obvious when BrMT and control currents are overlaid, as in Fig. 1 A, because BrMT increases the absolute time delay before channels open. To visualize the reduction of sigmoidicity by BrMT, I_K traces can be displayed on a timebase that has been normalized by the fitted time constant of activation. To do this, the timebase from each trace is divided by the value of τ from the fit of Eq. 1 (Fig. 1 C). This is similar to a scaling procedure used previously to quantitate delay before channel opening. (Zagotta et al., 1994b; Smith-Maxwell et al., 1998b; Kanevsky and Aldrich, 1999). After this transformation, the final phase of I_K rises at a similar rate in BrMT and under control conditions, but the smaller delay before I_K rise in BrMT is apparent.

The decrease in I_K sigmoidicity has implications for ShBΔ's gating in BrMT. Under control conditions, there is more sigmoidicity than could be produced by a single activation step occurring in each of the four subunits. In BrMT, sigmoidicity drops to $\sigma = 2$. This reduced sigmoidicity indicates that fewer activation steps are limiting the rate of I_K rise in BrMT. However, it is clear that all of ShBΔ's voltage-sensitive activation steps still occur when activation is slowed by BrMT; the total integral of ShBΔ gating charge movement is not altered when activation is slowed by BrMT (Sack et al., 2004). Thus, BrMT does not eliminate steps from the activation pathway, but instead decreases sigmoidicity by slowing some gating steps more than others. This agrees with what is already known, BrMT slows early steps in the activation path, making them rate limiting (Sack et al., 2004). Later steps that contribute to I_K sigmoidicity under control conditions are not slowed by BrMT, and thus contribute little to activation kinetics in BrMT.

Sigmoidicity Is Constant over a Wide Range of Voltages and BrMT Concentrations

BrMT reduces the sigmoidicity of ShBΔ activation to approximately $\sigma = 2$ under most conditions tested. This reduced sigmoidicity is retained at all voltages where the channels are maximally activated (Fig. 2). For example, in 5 μM BrMT, the sigmoidicity of ShBΔ activation is ~2 at activation voltages from 0 to +100 mV (Fig. 2 C). The constancy of sigmoidicity despite the changing activation rate indicates that in BrMT, all transitions contributing to I_K activation have the same voltage dependence. Otherwise, σ would change with

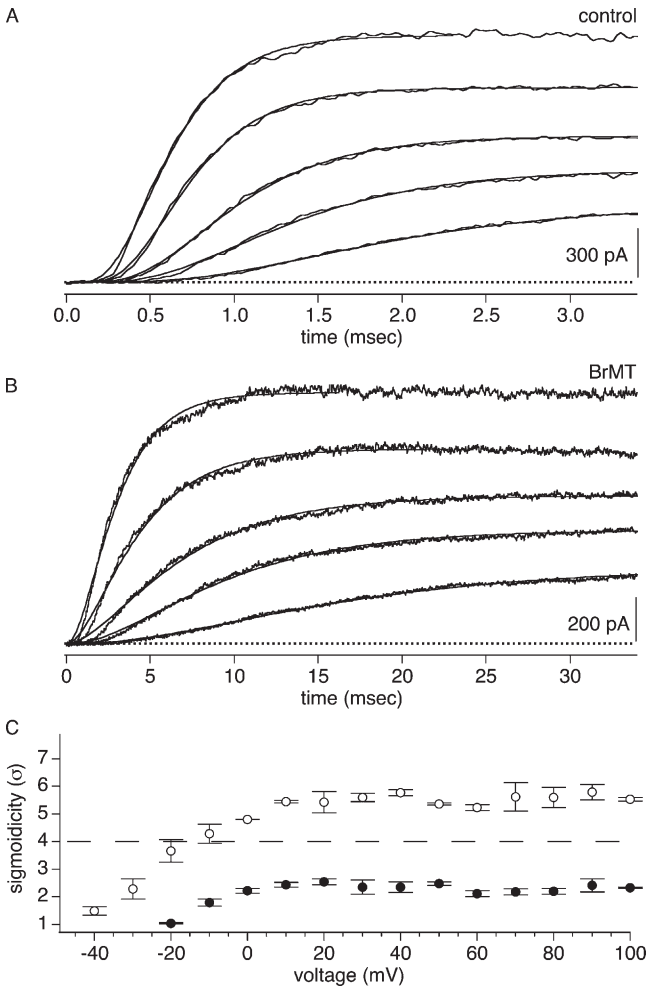

Figure 2. I_K activation waveforms from ShBΔ patches were fit with Eq. 1. (A) Fits of Eq. 1 to ShBΔ activation at 0, 20, 40, 70, and 100 mV. (B) Fits of Eq. 1 to activation in 5 μM BrMT. Same voltages as A. (C) Sigmoidicity from fits of Eq. 1 to I_K activation. Hollow circles, control condition; filled circles, 5 μM BrMT, $n = 4$ patches.

voltage as different voltage dependencies cause divergence of rates in the steps contributing to sigmoidicity. Activation steps that occur in multiple identical subunits have the same voltage dependence, suggesting that the sigmoidicty may be the result of slowing of the same activation step in different subunits.

The sigmoidicity of I_K in BrMT is also constant over a range of concentrations. As the concentration of BrMT is increased, activation is progressively slowed and peak I_K is reduced (Fig. 3 A). I_K sigmoidicity decreases from $\sigma = 6$ to near 2 (Fig. 3 B). BrMT has the same quantitative effect on I_K sigmoidicity from 2 to 20 μM. This constancy at $\sigma = 2$ indicates that ShBΔ activation is rate limited by the same steps at all these concentrations. This stability is in concordance with the mechanism proposed for BrMT action in which BrMT slows a specific early step in each subunit (Sack et al., 2004). In this mechanism, as BrMT concentration is increased, each subunit is slowed in an identically graded fashion.

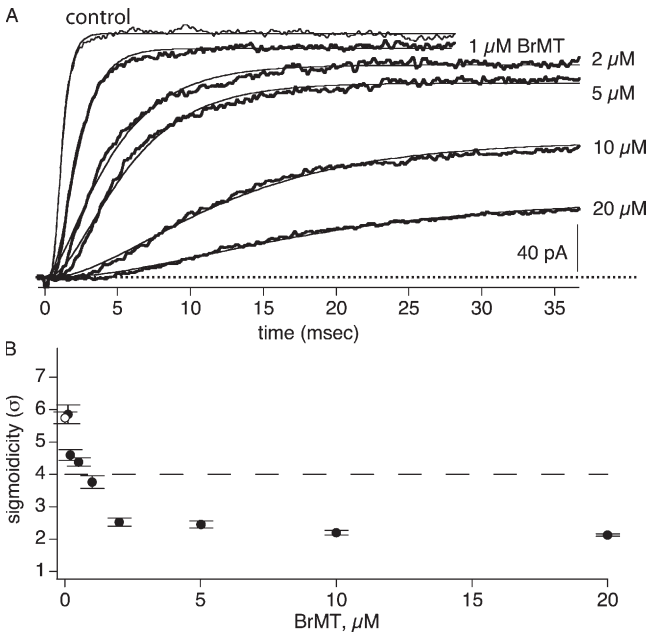

Figure 3. Sigmoidicity of activation approaches a value of 2 as BrMT concentration is increased. (A) ShBΔ I_K during voltage steps to +40 mV under control condition (thin trace) or 1, 2, 5, 10, and 20 μM BrMT (thick traces). Experimental I_K is average of multiple sweeps. Smooth lines are Eq. 1 fit to I_K. (B) Sigmoidicity from fits of Eq. 1 to activation at +40 mV, n = 3–5 patches.

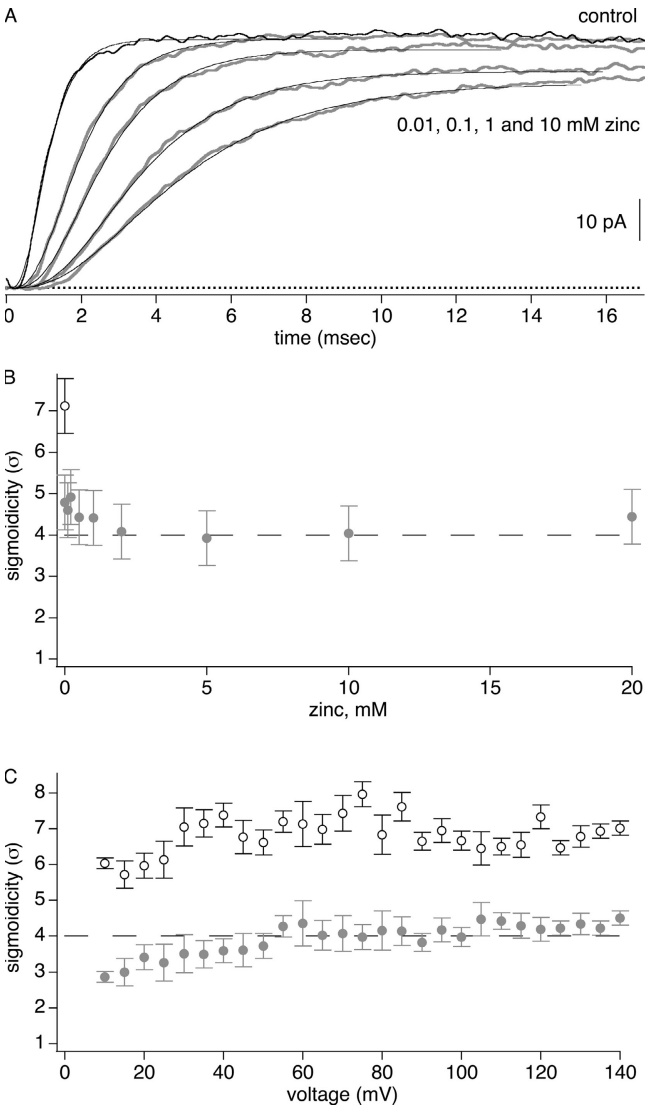

Figure 4. Divalent zinc reduces ShBΔ sigmoidicity to σ = 4. These experiments used the pH 6.8 external solutions described in Materials and Methods. (A) ShBΔ I_K activated at +60 mV in 0, 0.01, 0.1, 1, and 10 mM zinc. Smooth thin lines are fits of Eq. 1 to data. (B) Sigmoidicity under control condition (hollow circle) or with added zinc (gray circles), n = 5–8 patches. (C) Sigmoidicity of I_K is constant over a wide voltage range. In 2 mM zinc, sigmoidicity is ∼4 (gray circles), n = 5 patches. Control sigmoidicity is >4 (hollow circles), n = 3 patches.

The constant sigmoidicity of activation over a wide range of BrMT concentrations and voltages suggests that the same gating steps determine the time course of activation under all these conditions. The perplexing question is how can slowing early gating steps lead to I_K with a sigmoidicity of 2? Early gating steps are supposedly independent in each subunit (see INTRODUCTION). Independence demands that I_K have a sigmoidicity of $\sigma \geq 4$. This sigmoidicity of $\sigma < 4$ requires that early steps cooperate when slowed by BrMT. Is this low sigmoidicity a hallmark of intrinsically cooperative early steps that are slowed by BrMT, or does BrMT somehow alter the cooperativity of early steps to lower their sigmoidicity?

Sigmoidicity Analysis Suggests Zinc Slows Independent Activation Steps

To better understand the reduction of ShBΔ sigmoidicity by BrMT, sigmoidicity was analyzed with another ligand that slows ShBΔ activation in a similar fashion. Like BrMT, many divalent transition metal ions slow K channel activation in a graded fashion (Gilly and Armstrong, 1982; Terlau et al., 1996; Elinder and Arhem, 2003). Of these gating modifier ions, divalent zinc is among the most potent and the best characterized gating modifier of Shaker-type K channels, making it a good choice for study (Gilly and Armstrong, 1982; Spires and Begenisich, 1994; Yellen et al., 1994; Zhang et al., 2001). Like BrMT, zinc slows ShBΔ activation in a progressive manner, with increasing concentrations of zinc leading to greater slowing of I_K rise (Fig. 4 A). When slowed by zinc, ShBΔ's sigmoidicity is quite different than when slowed by BrMT. In zinc, σ = 4 at all concentrations that slow activation (Fig. 4 B). In zinc, sigmoidicity is also constant at σ = 4 over a wide voltage range (Fig. 4 C). This sigmoidicity of σ = 4 is what would be expected if zinc slowed one independent step in each subunit. The sigmoidicity of activation in zinc suggests that zinc slows early steps in the ShBΔ activation path that are independent among subunits.

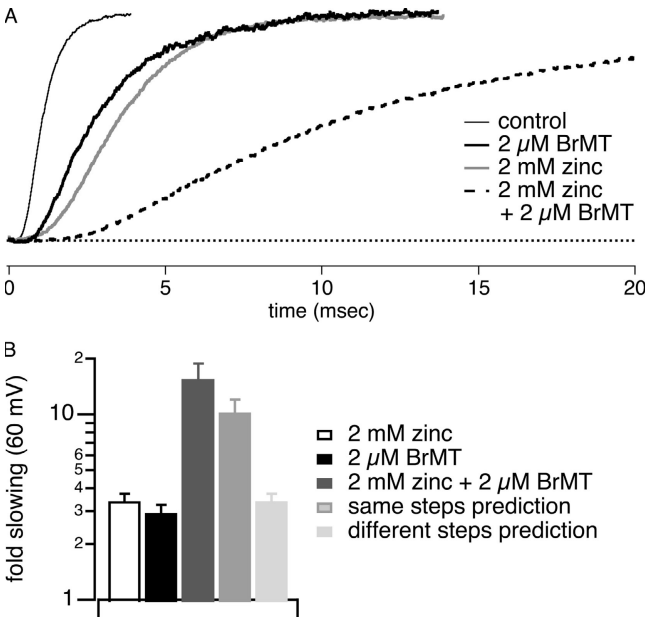

Figure 5. BrMT and zinc slow the same activation steps, yet induce different sigmoidicities. The pH 6.8 solutions described in Materials and Methods were used for experiments in this figure. (A) I_K at +60 mV during application of BrMT and/or zinc. Traces are scaled to match peak I_K. (B) Slowing induced by zinc and/or BrMT was determined from τ in fits of Eq. 1, $n = 4$. The light gray bar is the multiplicative product of the fold-slowing in 2 mM zinc and 2 μM BrMT. This predicts the degree of slowing expected from both ligands together if they both slow the same activation step. The speckled bar is the degree of slowing expected if BrMT and zinc slow different activation steps: the combined slowing would be no more than the slowest of the two alone, in this case, zinc.

Zinc and BrMT Slow the Same Gating Steps

The sigmoidicity of ShBΔ I_K of $\sigma = 4$ in zinc is distinct from $\sigma = 2$ in BrMT. The different sigmoidicities induced by the two ligands could be interpreted in two basic ways. Either BrMT slows different activation steps than zinc and these steps have different cooperative interactions between subunits, or BrMT slows the same activation steps as zinc but alters intersubunit cooperativity. To distinguish between these two possibilities, simultaneous application of BrMT and zinc was examined. If BrMT slows different activation steps than zinc, then a concentration of BrMT that slows activation say, fourfold, should have little effect on activation rate when I_K is already slowed fourfold by zinc. Thus, if BrMT and zinc slowed different steps, activation with both would not be much slower than either of the gating modifiers separately.

Experimentally, we find that BrMT and zinc applied together slow activation very much more than either ligand alone (Fig. 5 A). This indicates that both ligands must slow the same activation steps. If the ligands slow the same activation steps in a noncompetitive fashion, the slowing of activation should be the product of the slowing factors of each ligand, e.g., if BrMT slows activation fourfold, and zinc fourfold, then simultaneous application would slow activation 16-fold. This simple, noncompetitive model of inhibition predicts the degree of slowing seen experimentally (Fig. 5 B). When both zinc and BrMT are applied, the degree to which activation is slowed is close to the product of the two alone. This clearly demonstrates that zinc and BrMT slow the same steps in ShBΔ's activation pathway.

What does coapplication of zinc and BrMT tell us about the cooperativity of these early steps? When coapplied, zinc and BrMT slow the same activation steps, but the sigmoidicity of BrMT dominates. I_K sigmoidicity in simultaneous zinc and BrMT is close to what would be expected with BrMT alone, $\sigma = 2.3 \pm 0.2$ ($n = 4$). This means that although activation of these early steps continues to occur independently in zinc, addition of BrMT imbues these slowed early steps with intersubunit cooperativity.

The conclusion that BrMT induces cooperative activation of otherwise independent early steps is consistent with the known properties of early activation in ShBΔ channels. Many other studies have concluded that early steps occur independently in each subunit (Smith-Maxwell et al., 1998b; Kanevsky and Aldrich, 1999; Ledwell and Aldrich, 1999; Horn et al., 2000; Mannuzzu and Isacoff, 2000; Pathak et al., 2005). The observation here that zinc-slowed ShBΔ I_K has a sigmoidicity of $\sigma = 4$ is additional evidence that the affected early steps are independent among subunits. The ability of BrMT to reduce sigmoidicity to $\sigma = 2$, with or without zinc, forces us to conclude that BrMT induces cooperativity in early gating steps. To bring about cooperativity amongst independent ShBΔ gating steps, BrMT must itself bind cooperatively.

BrMT Induces Cooperativity by an Allosteric Mechanism

To bind cooperatively to ShBΔ channels, a bound BrMT could alter the binding of BrMT directly, with BrMT molecules on different subunits physically interacting with one another, or indirectly, by causing a conformational change in the channel protein. For a bound BrMT to directly affect BrMT binding at an equivalent site on another subunit, BrMT would need to bind near the central axis of the K channel. BrMT is quite small relative to a Shaker subunit. Single particle EM reconstructions of the Shaker channel show the channel to be ~100 Å in diameter (Sokolova et al., 2001), and the crystal structure of the closely related Kv1.2 channel is 95 Å in diameter (Long et al., 2005a). A BrMT dimer is the size of a dipeptide, possibly 10 Å in its most outstretched conformation. A BrMT molecule could sterically block an equivalent binding site on another subunit, if its binding site spans the same location on two subunits of the Shaker channel. To sterically prevent binding to a neighboring subunit, a simple pythagorean analysis finds that BrMT would have to bind

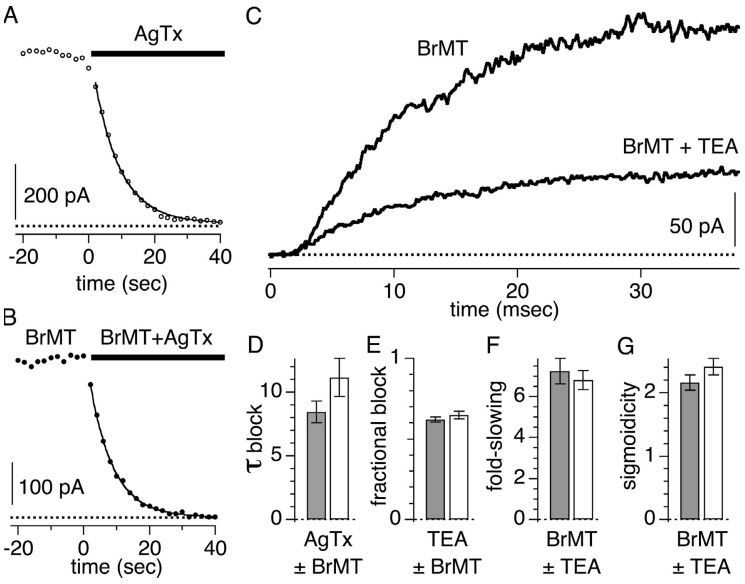

Figure 6. BrMT does not compete with ligands that block the external pore of ShBΔ channels. All data were measured during 50-ms pulses to +40 mV given every 2 s. Blockers were applied by manually triggering solution switching during the interval between pulses. Solution exchange requires <1 s. (A) Circles are peak ShBΔ I_K, measured by averaging over several milliseconds after a steady-state level of I_K activation. At time = 0, 50 nM agitoxin-2 is added to the external solution. (B) Same as A, but with 5 μM BrMT in all solutions. (C) Block of ShBΔ I_K by 1 mM TEA in the presence of 5 μM BrMT. (D) Mean time constant of block by 50 nM agitoxin-2 with 5 μM BrMT (gray bar, $n = 6$ patches), and without BrMT (white bar, $n = 5$ patches). (E) Mean block by 1 mM TEA with 5 μM BrMT (gray bar, $n = 6$ patches), and without BrMT (white bar, $n = 9$ patches). (F) Mean fold-slowing of activation by 5 μM BrMT with 1 mM TEA (gray bar) and without TEA (white bar). ShBΔ I_K was fit by Eq. 1, and the fold-slowing is the ratio of τ in BrMT to τ before addition of BrMT. (G) Gray bar is sigmoidicity of ShBΔ I_K in 5 μM BrMT with 1 mM TEA (gray bar) and without TEA (white bar).

within 7 Å of the channel's central axis of symmetry. As BrMT is effective only from the external side of the membrane (Sack et al., 2004), a direct mechanism of cooperative interaction would require that BrMT bind in the external "turret" region surrounding the pore of K channels (Doyle et al., 1998). To determine whether BrMT binds near the external end of the channel pore, we made measurements to see if BrMT competes with ligands that bind in this turret region.

BrMT does not inhibit the binding of agitoxin-2. The agitoxin continued to bind the T449Y variant of the ShBΔ K channel at a similar rate in the presence of BrMT (Fig. 6, A, B, and D). The agitoxin actually bound slightly faster during experiments with BrMT in solution. This indicates that BrMT does not bind near the channel pore, as bound agitoxin radially extends ∼15 Å from the center of the ShBΔ channel (Hidalgo and MacKinnon, 1995; Krezel et al., 1995; Gross and MacKinnon, 1996; Ranganathan et al., 1996; Eriksson and Roux, 2002). This lack of competition also suggests that BrMT binds far from the turret region, as the two amines of BrMT would be expected to electrostatically repel the positively charged agitoxin if BrMT bound within a debye length (∼10 Å) of any basic toxin residue.

This conclusion that BrMT does not bind near the pore was corroborated by the lack of competition between BrMT activity and tetraethyl ammonium (TEA) block (Fig. 6, C, E, F, and G). External TEA blocks ShBΔ K conductance by binding at the mouth of the K pore (MacKinnon and Yellen, 1990; Lenaeus et al., 2005). In the Shaker variant used here, the TEA binding site is formed by a tyrosine residue (T449Y) from each of the four subunits in this channel (Heginbotham and MacKinnon, 1992). TEA is a rapid blocker of ShBΔ K channels that reduces their measured single channel current. BrMT does not reduce single channel I_K nor does BrMT affect ShBΔ channels in any other appreciable way after they open during a positive voltage step (Sack et al., 2004). Thus it would be surprising if BrMT affects TEA block of channels. Unshockingly, BrMT does not inhibit TEA block (Fig. 6, C and E). More telling is the lack of an effect of TEA on BrMT-induced I_K slowing. BrMT slows activation equally well in the presence or absence of 1 mM TEA. When Eq. 1 is fit to I_K activation in BrMT, no TEA effect is seen on either the time constant or sigmoidicity associated with activation.

The spatial constraints placed by a lack of competition between BrMT and pore blockers indicates that BrMT does not bind near the external K channel pore. Thus, the cooperativity of BrMT binding cannot be due to direct interaction between molecules bound to different subunits. Rather, the cooperativity of BrMT binding must be allosteric in nature, due to a change of conformation in the K channel subunits.

Cooperativity in BrMT Binding

There are many different cooperative mechanisms by which ligands can bind to subunits of a protein. Here we attempt to flesh out the simplest binding mechanism that can account for the effects of BrMT on ShBΔ gating, making use of the previous finding that subunit activation greatly decreases BrMT affinity (Sack et al., 2004). We start by addressing different classes of binding schemes.

Independent Binding. If BrMT independently bound each subunit to slow an early activation step, these slowed early steps would remain independent in each subunit. Then I_K would have a sigmoidicity of $\sigma = 4$, as it does when slowed by zinc, instead of the sigmoidicity of $\sigma = 2$ observed experimentally. Thus, BrMT cannot bind to each subunit independently.

Positively Cooperative Binding. If BrMT bound in a positively cooperative fashion, then after one BrMT molecule binds, other subunits are more likely to bind BrMT. With strong positive cooperativity, BrMT would only effectively slow one transition along the activation path, because once a subunit activates and casts off its BrMT, the positive cooperativity of binding would cause others to immediately follow suit. This would give BrMT-treated I_K a sigmoidicity of $\sigma = 1$, that of a single exponential rise. This is clearly different from the observed value of $\sigma = 2$.

Negatively Cooperative Binding. In a negatively cooperative process, a ligand binding to one subunit inhibits ligand binding to other subunits. Three simple cases of negative cooperativity could exist in a tetramer: (1) binding to one subunit prevents binding to the other three, (2) binding to two subunits prevents binding to the other two, and (3) binding to three subunits prevents binding to the other one.

The implications of these binding schemes for sigmoidicity are fairly straightforward. (1) If an independent early step is slowed by BrMT binding to only one subunit of the channel, then I_K sigmoidicity will approach $\sigma = 1$. (2) If an independent early step is slowed by BrMT binding to two subunits of the channel, then I_K sigmoidicity will approach $\sigma = 2$. (3) If an independent early step is slowed in three subunits of the channel, then I_K sigmoidicity will approach $\sigma = 3$.

Of all these cooperative binding schemes, only the negatively cooperative binding scheme where only two subunits bind BrMT gives I_K sigmoidicity a value of $\sigma = 2$. A sigmoidicity of 2 is suggestive of only two of the four subunits being rate limiting for activation. How would this occur in a rotationally symmetric K channel? The most plausible answer is that BrMT molecules bind two subunits diagonally opposed to each other. This would be caused by a subunit that binds BrMT, preventing its adjacent neighbors from binding BrMT. The two free subunits would activate rapidly, leaving two resting subunits inhibited by BrMT. This simple scheme can explain the sigmoidicity of $\sigma = 2$ induced by BrMT, and is modeled in detail below.

A Negatively Cooperative Model of BrMT Inhibition

Modeling BrMT Effects on Activation. The degree of slowing produced by BrMT can be calculated using a previously developed model of strong negative allosteric coupling between BrMT binding and activation of a subunit (Sack et al., 2004). Put simply, a subunit cannot activate when BrMT is bound. The degree to which BrMT slows activation in an individual resting subunit is determined by the probability that BrMT is bound to that subunit at equilibrium:

$$b = 1 - pBrMT. \tag{2}$$

Here b is the coefficient by which the activation rate of an individual subunit is slowed. The factor $pBrMT$ is the probability that BrMT is bound to a resting subunit, assuming that BrMT binding is at equilibrium. If a subunit activates with a rate α under control conditions, then it will activate with a rate $b \cdot \alpha$ in BrMT. As the concentration of BrMT is raised and the probability of a subunit binding BrMT increases, b approaches zero and activation is infinitely slowed. As the concentration of BrMT is reduced to nothing, b approaches one and activation returns to its control rate.

To model BrMT binding individual subunits of the K channel, BrMT binding is summarized by an equilibrium constant (K_{eq}) for binding. K_{eq} is the ratio of bound to unbound subunits and is determined from the concentration of BrMT and its dissociation constant for a ShBΔ subunit (K_D):

$$K_{eq} = \frac{pBrMT}{1 - pBRMT} = \frac{[BrMT]}{K_D}. \tag{3}$$

We represent binding of BrMT by the appearance of the letter B on a channel subunit:

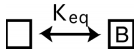

(SCHEME 2)

Negatively Cooperative Binding. To model two BrMT molecules binding to a tetrameric K channel, we develop a model where BrMT is disallowed from simultaneously binding any two adjacent subunits. In this case the probability of BrMT binding is affected by a simple algebra.

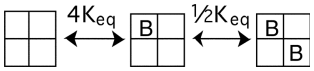

(SCHEME 3)

Scheme 3 depicts a model where BrMT binds only two diagonal subunits in a fourfold symmetric channel. The macroscopic equilibrium constant for each binding event is determined by the number of subunits available to bind or unbind BrMT. As there are four subunits available to bind the first BrMT, the probability of binding one BrMT will be $4K_{eq}$, four times the equilibrium constant of a single binding event. Once a single BrMT is bound, there is only one diagonal subunit available to bind a second BrMT, but two BrMT molecules available to unbind in the reverse direction. Therefore the equilibrium for the second binding event is $1/2K_{eq}$.

To build a complete model of activation in BrMT, binding equilibria must be determined for each state along the activation pathway. Although Scheme 3 is a complete BrMT binding scheme for a channel with all subunits resting, BrMT binds differently to different activation states. Activation greatly decreases a subunit's affinity for BrMT. BrMT stabilizes resting states, and activated channels behave as if they no longer bind BrMT (Sack et al., 2004). The following schemes depict the

relevant binding equilibria for states along the activation path with different sets of activated subunits.

If one subunit activates, and that subunit no longer binds BrMT, the equilibria for BrMT binding to other subunits of the channel are then:

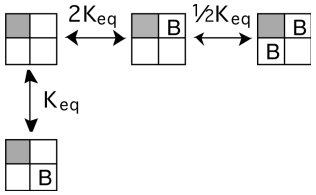

(SCHEME 4)

With one voltage sensor activated (grayed subunit in a Scheme 4), the only way for two BrMT ligands to bind is if they are both adjacent to the activated subunit.

The second voltage sensor to activate can be either adjacent or diagonal to the first one.

(SCHEME 5)

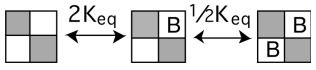

(SCHEME 6)

These two cases behave quite differently. When an adjacent subunit activates, as in Scheme 5, BrMT can only bind to one of the two resting subunits. Hence, at least one subunit will always be unencumbered by BrMT. In Scheme 6, both resting subunits can bind BrMT, and resting subunits in this state will be encumbered by high concentrations of BrMT.

Once three subunits activate, the remaining resting subunit can bind BrMT and the final subunit to activate will always be retarded by high concentrations of BrMT.

(SCHEME 7)

Note that of these schemes, only in Schemes 6 and 7 are all resting voltage sensors simultaneously available to bind BrMT. These states are important to the final kinetic model, because it is these two states that activate most slowly and endow I_K in BrMT with a sigmoidicity of $\sigma = 2$.

Activation Gating

To determine how much BrMT slows activation transitions from each of the states above, the connectivity of these states needs to be formalized. When four identical subunits activate independently, their behavior can be summarized in a linear scheme where

(SCHEME 8)

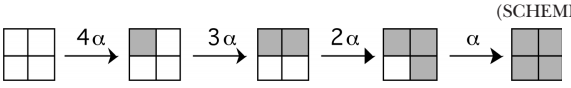

This model of independent activation is mathematically simplified by the channel's fourfold symmetry. To accommodate BrMT binding to only two of the four subunits, more states must be added to Scheme 8. BrMT is disallowed from binding to adjacent subunits, so adjacent subunits need to be distinguished from diagonal subunits (see Schemes 5 and 6). Scheme 8 can be modified to treat adjacent and diagonal subunits differently, by expanding the state with two activated voltage sensors such that adjacent and diagonal activation is considered separately:

(SCHEME 9)

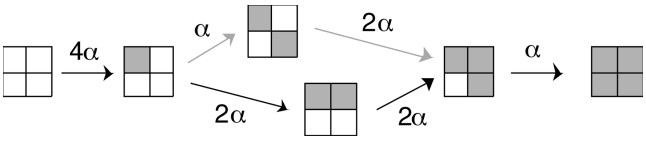

Note that without BrMT, Scheme 9 collapses to Scheme 8. This is because the rate of activating a second subunit is $2\alpha + \alpha = 3\alpha$, and the rate of activating a third subunit is 2α from either state with two subunits activated.

When BrMT is added, each transition in Scheme 9 will be slowed to a different degree. The slowing cofactor for each transition is determined by how often BrMT is bound to each subunit, which is detailed in Schemes 3–7. Calculating the effects of BrMT on the transitions in Scheme 9 involves the following: (a) finding pBrMT for each subunit and calculating how much the BrMT binding slows the activation of that subunit; and (b) summing the BrMT slowed activation rates for every subunit available to activate.

Fig. 7 schematizes the effects of BrMT binding equilibria on the activation path from Scheme 9. For each activation transition, the effects of BrMT binding can be summarized by a single cofactor. This scheme creates a framework from which the effects of BrMT slowing the activation of a homotetrameric channel can be simulated.

A Complete BrMT Activation Model. Accurately modeling ShBΔ I_K involves implementing more than one activation step per subunit (Zagotta et al., 1994b; Schoppa and Sigworth, 1998c). To simulate the effects of BrMT on ShBΔ I_K, we add BrMT slowing factors into an established gating model. BrMT binding is incorporated into the ShBΔ activation model of Zagotta et al. (1994a; model ZHA). Model ZHA accurately reproduces the ionic currents, gating currents, and single channel behavior of ShBΔ channels in the voltage regime studied here. In model ZHA, all four subunits transition through two activation steps apiece before the open state is reached. All transitions, aside from the closing step, are independent among the identical subunits.

BrMT has been found to exclusively slow forward transitions early in ShBΔ's activation path (Sack et al., 2004). In model ZHA, each of the four identical subunits traverse one early and one late activation step.

We implement BrMT slowing into model ZHA by allowing BrMT to inhibit only the early activating transition in individual subunits (Fig. 8 A). Schematizing this inhibition on a single subunit is simple, but the scheme becomes more complex when the entire channel is taken into account. The expansion of the ZHA model to accommodate BrMT binding creates many new states (Fig. 8 B). This model may appear daunting, but it is actually just a logical expansion of the model in Fig. 7. The slowing factors, b_1–b_6, are determined by a single free parameter, a subunit's K_D for BrMT. This is the only new free parameter required to model BrMT inhibition in model ZHA, and K_D is determined without measuring sigmoidicity. In a previous paper we used activation kinetics to assign a K_D of 0.8 μM for BrMT binding to resting subunits of the ShBΔ channel (Sack et al., 2004). Remarkably, inserting this independently derived K_D into model ZHA produces sigmoidicities similar to experiments (Fig. 9). As BrMT concentration is increased, the modeled I_K asymptotically approaches a sigmoidicity of ∼2 (Fig. 9 E). Importantly, the modeled currents lose sigmoidicity with a dose–response similar to that seen experimentally. Perhaps even more telling is the model's prediction of sigmoidicity versus activation slowing (Fig. 9 F). Both the sigmoidicity of activation and its underlying time constant are determined by the amount of BrMT bound. Therefore the relationship between degree of activation slowing and sigmoidicity is independent of the channel's affinity for BrMT. The similarity between simulation and experiment in Fig. 9 F is set by model ZHA, without any new free parameters being fitted, the values of these parameters were determined before BrMT was ever discovered. This shows that this class of model, with two subunits predominantly slowed by BrMT, is likely correct.

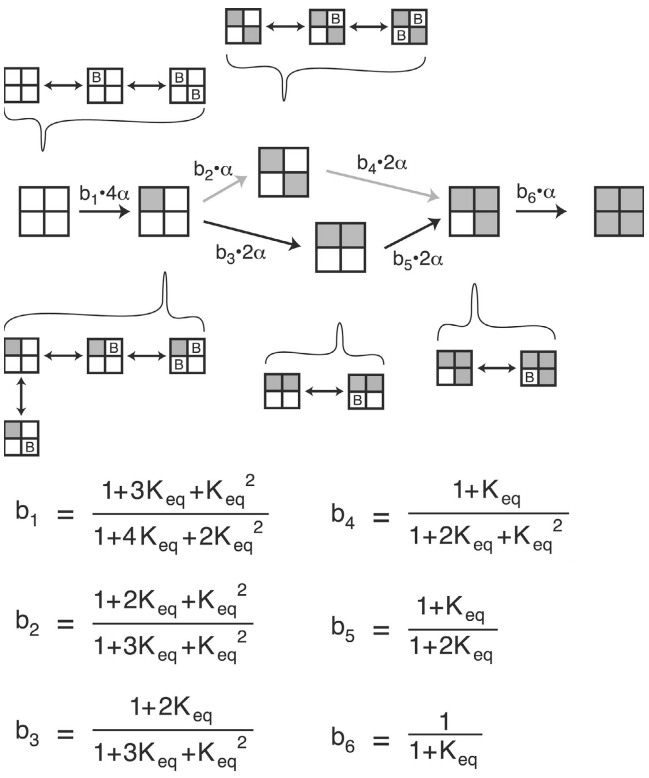

$$b_1 = \frac{1+3K_{eq}+K_{eq}^2}{1+4K_{eq}+2K_{eq}^2} \qquad b_4 = \frac{1+K_{eq}}{1+2K_{eq}+K_{eq}^2}$$

$$b_2 = \frac{1+2K_{eq}+K_{eq}^2}{1+3K_{eq}+K_{eq}^2} \qquad b_5 = \frac{1+K_{eq}}{1+2K_{eq}}$$

$$b_3 = \frac{1+2K_{eq}}{1+3K_{eq}+K_{eq}^2} \qquad b_6 = \frac{1}{1+K_{eq}}$$

Figure 7. Schematic depicting the relevant states in an activation path involving one activating transition per subunit. In this model, BrMT simultaneously binds two of the four subunits to slow activation. The forward transition is set by the effect of the BrMT's slowing factor, b_x, on the activation rate constant α. The slowing coefficient of each transition (b_1–b_6) is determined from the probability that BrMT is bound to individual resting subunits. K_{eq} is the binding equilibrium for BrMT.

For rate α, at positive voltages, the experimental sigmoidicity of I_K activation under control conditions was lower than that predicted by model ZHA. On average, I_K sigmoidicity was ∼6 at +40 mV, while model ZHA simulates a sigmoidicity of ∼7. In model ZHA, sigmoidicity is highest when forward transitions α and γ occur at equal rates. We suspect the presence of 2 mM calcium in our external solution may have slowed the first activation transition. Zagotta et al. (1994) did not use calcium, and we have shown here that divalent ions can slow the first activating transition. Hence, in model BrMT, α was slowed to 76% of model BrMT's ZHA rate to reduce sigmoidicity to experimental values.

For factor θ and rate δ, at negative voltages where not all of ShBΔ's voltage sensors activate, experimental I_K has less sigmoidicity than model ZHA. This again could be due to differences between solutions used by Zagotta et al. and solutions used here. At low voltages, sigmoidicity is determined by the transitions with the slowest rate, here 4δ/θ, the first deactivation step in each subunit. To alter sigmoidicity at low voltages, the value of θ was increased, while keeping the rate of the first closing step constant, by multiplying δ by same amount as θ. Tripling the value of θ and δ to 30 provided the right amount of sigmoidicity at low open probability. This is within the range of θ values that was previously shown to fit ShBΔ ionic and gating currents (Zagotta et al., 1994a).

For slowing factors b_1–b_6, the voltage range where channels begin to open in BrMT is slightly too negative in model ZHA. To correct this, the assumption that BrMT only affects forward transitions was relaxed. In model BrMT, BrMT accelerates β reverse transitions by the same degree it accelerates forward ones. This modification indicates that the activated voltage sensors are destabilized by BrMT just as resting voltage sensors are stabilized by BrMT.

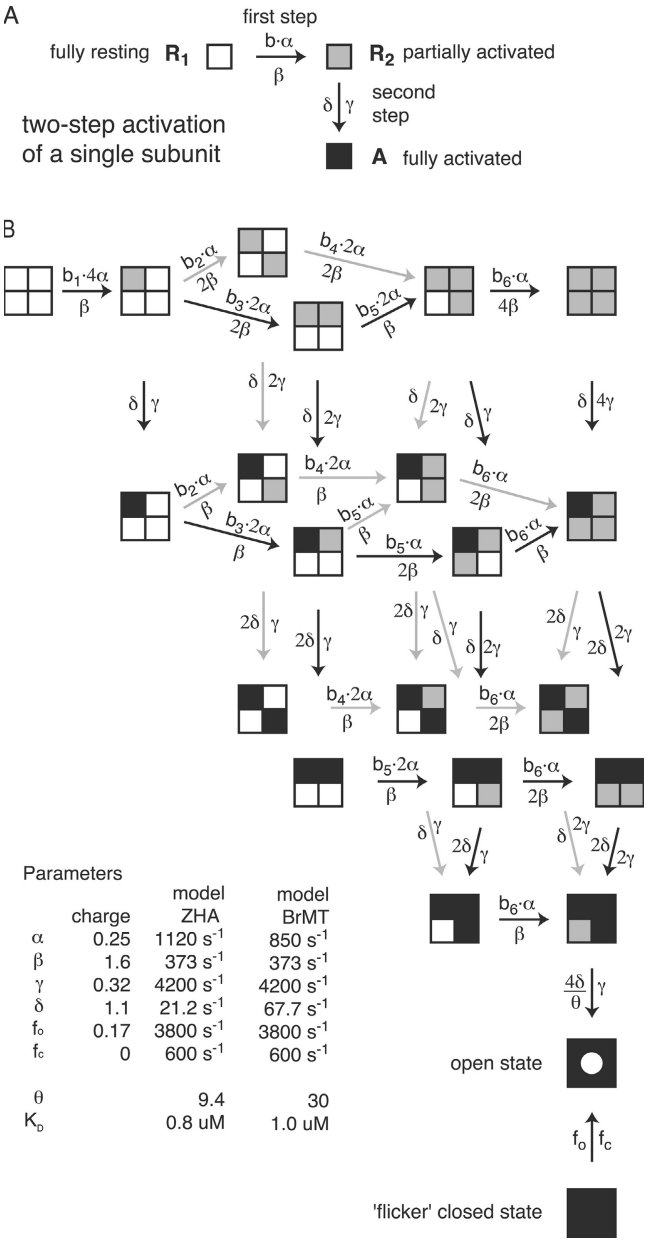

Figure 8. Model of negative cooperative inhibition of ShBΔ activation. (A) Depiction of activation in a single subunit. Each subunit completes two activation steps. Forward transitions toward the open state are marked by a darkening of the subunit from white to gray in the first step and then gray to black in the second step. The first forward transition is set by the effect of the BrMT's slowing factor, b, on rate constant α, the reverse by β. The second forward transition has rate γ, and the reverse δ. In model BrMT, the reverse transition, β, is accelerated by a factor 1/b. (B) A model for implementing negatively cooperative binding of BrMT, such that it slows an early step in the Shaker activation pathway. The model is an elaboration of the ShBΔ activation model of Zagotta et al. (1994a). White subunits are available to bind BrMT. Vertical transitions are not affected by BrMT. The open state is demarcated with a hollow circle. The bottom-most is the "flickery" closed state. Equations for the BrMT slowing factors (b_1–b_6) are shown in Fig. 7. In model BrMT, all reverse transitions (those involving β) are accelerated by the inverse of the factor that slows the forward transition. This model does not attempt to account for the reduction of peak I_K by BrMT.

With these parameters altered, the kinetics and voltage dependence of activation BrMT are greatly improved, and a functional model of BrMT effects on ShBΔ activation kinetics is established. The dose–response effects of BrMT are not much changed by the modifications made in model BrMT (Fig. 9), but the exact kinetics and voltage dependence of I_K rise are better simulated. Eq. 1 systematically errs at the foot of I_K rise, and model BrMT better reproduces experimental I_K (Fig. 10 A). The modifications to model ZHA allow simulated I_K rise to match experimental data over a wide voltage range. Fig. 10 B demonstrates the accuracy to which model BrMT predicts I_K activation amplitude and waveform over the range of voltages. This model was not directly fitted to sigmoidicity in BrMT, but does a remarkable predictive job at different voltages (Fig. 10 C). The most variable factor in model BrMT was found to be the K_D for BrMT. The effect of BrMT varied greatly from patch to patch. We suspect that membrane partitioning of BrMT leads to the variability in its apparent K_D.

These fits are still not perfect, and can be improved further by altering more parameter values and/or adding new parameters to the model. Models with different reverse transitions could improve fits to sigmoidicity at low open probability. Allowing neighboring subunits to bind BrMT with a reduced affinity improved fits to some of the experimental data, but this requires a more complex model with at least one additional free parameter. Likewise, other models with different mechanisms of negative cooperativity in BrMT binding might also improve fits, but further model expansion was deemed not to be justified. The number of subtle variations that could be made are infinite while the data we have to fit are finite. Model BrMT reproduces the effects of BrMT on ShBΔ I_K, and most importantly, it demonstrates that negatively cooperative BrMT binding can account for the sigmoidicity seen experimentally.

DISCUSSION

Physical Interpretations of Negative Cooperativity in Binding

Dimer of Dimers? The negatively cooperative mechanism described here requires that the fourfold rotational symmetry of the channel itself be broken: two subunits bind BrMT while the other two do not. This mode of functioning has been suggested for ligand binding to other related homotetrameric channels, such as glutamate receptors (Sun et al., 2002), small conductance calcium activated channels (Schumacher et al., 2001), and cyclic nucleotide-gated channels (Root and MacKinnon, 1994). The proposed mechanism for BrMT action suggests that voltage-gated K channels can also operate as a dimer of dimers under the appropriate conditions.

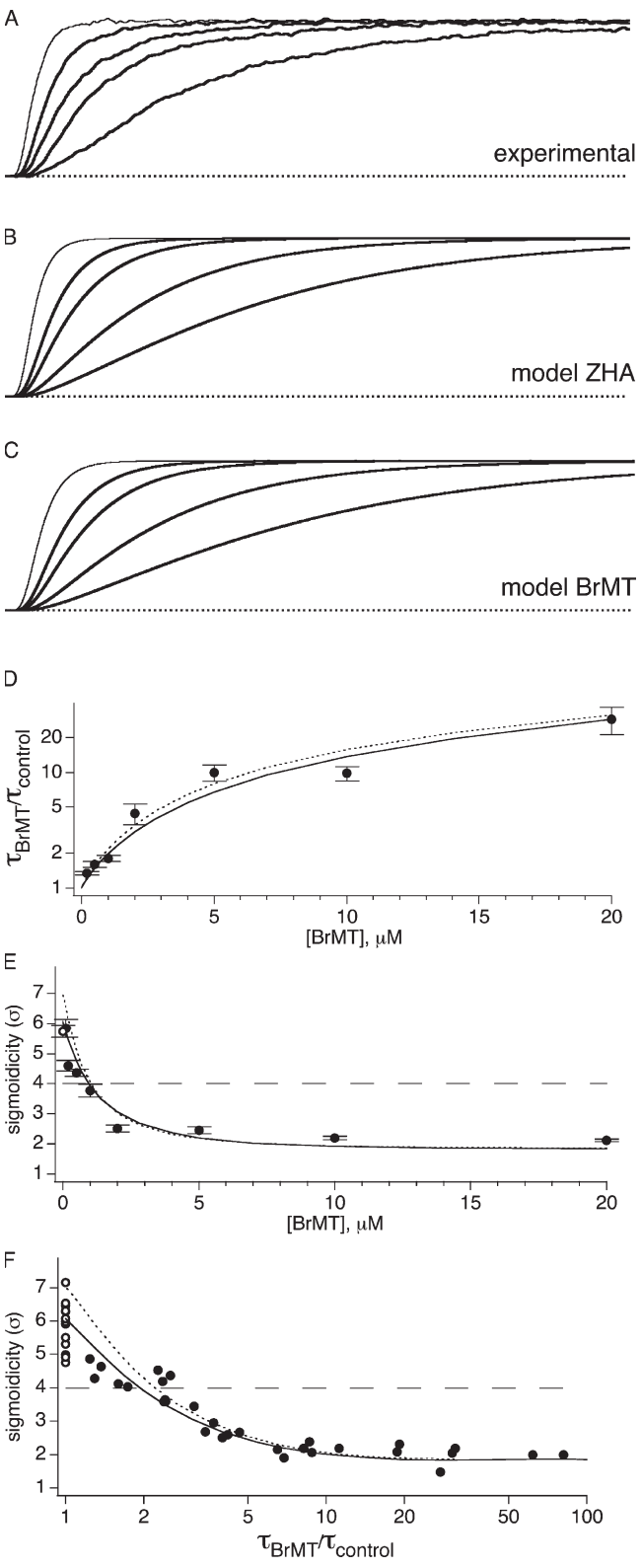

Figure 9. Effects of BrMT on simulated and experimental I_K from ShakerBΔ. The negatively cooperative models used for simulations are depicted in Fig. 8 B. (A) ShBΔ I_K from an outside-out patch upon activation to +40 mV. Thin line, control condition (no BrMT); thick lines, 1, 2, 5, and 10 μM BrMT. I_K was normalized to match peak current level. (B) Simulated ShBΔ currents from model ZHA. Thin line, control condition; thick lines, 1, 2, 5, and 10 μM BrMT. (C) Simulated ShBΔ currents from model BrMT. Thin line, control condition; thick lines, 1, 2, 5, and 10 μM BrMT. (D) Filled circles, fold slowing of ShBΔ activation at +40 mV by BrMT, n = 4–9 patches; dotted line, model ZHA; solid line, model BrMT. (E) Filled circles, sigmoidicity of ShBΔ I_K at +40 mV, n = 3–5 patches; hollow circle is control condition; dotted line, model ZHA; solid line, model BrMT. (F) Sigmoidicity of I_K vs. slowing by BrMT. Each data point is a measurement in control solution (hollow circles), or a solution containing 0.5–20 μM of BrMT (filled circles). Dotted line, model ZHA; solid line, model BrMT.

Cooperativity among Separated Domains. A voltage-sensitive K channel can be treated as having two separable domains: the voltage-sensing S1–S4 region of the channel, and the S5–S6 pore domain (Lu et al., 2001; Murata et al., 2005; Ramsey et al., 2006). In a crystal structure of the Kv1.2 channel, the S1–S4 regions of the channel hang off the edges of the S5–S6 (Long et al., 2005a,b). The S1–S4 region does not contact the S1–S4 in other subunits, a structure physically consistent with claims that early voltage sensor movement occurs independently in each subunit. BrMT must affect the structure of this region, because BrMT inhibits voltage activation. It is not known where BrMT binds, but the cooperativity of BrMT binding indicates that structural changes upon BrMT binding must extend beyond the physically separated S1–S4 region of each subunit. One option is for BrMT to induce the S1–S4 region of two subunits to contact one another, but this seems unlikely because these domains are separated by >20 Å in its crystal structure. More likely, BrMT alters the conformation of the S5–S6 region, as this region has a large number of intersubunit contacts. This means that without moving the residues of the pore and external turret region that comprise the agitoxin-2 binding site, BrMT must induce a conformational change to affect BrMT binding in adjacent subunits.

Implications of Induced Cooperativity

We have found a ligand that induces cooperativity among subunits that normally activate independently of one another. The induction of cooperative activation by BrMT is due to negatively cooperative binding of the ligand. In our model, occupation of one subunit by BrMT prevents occupation of adjacent subunits by BrMT. The cooperative binding of BrMT creates a means by which normally independent subunits influence each other during activation. According to the model introduced here, when a subunit binds BrMT, negative cooperativity prevents adjacent subunits from binding BrMT, and thus its neighbors are less retarded by BrMT. Thus, cooperative BrMT binding induces cooperative activation. The model proposed here is the simplest we found to account for the sigmoidicity measured in BrMT. A more complex model involving more free parameters might produce similar results,

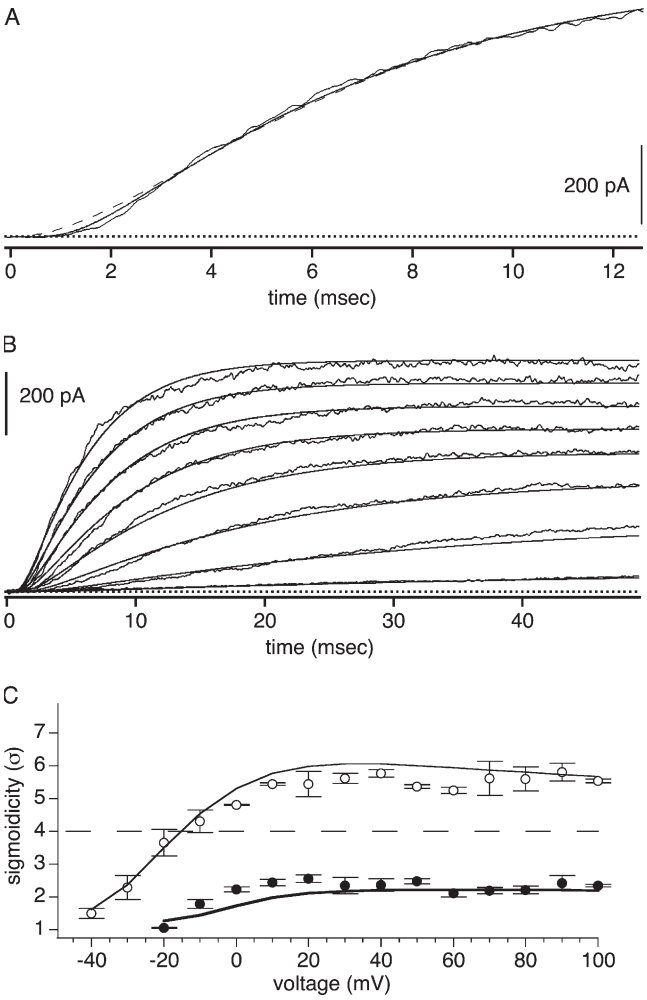

Figure 10. Voltage dependence of cooperative binding model BrMT. (A) Noisy line, experimental I_K at +40 mV in 5 μM BrMT; smooth line, activation of model BrMT at +40 mV in 5 μM BrMT; dashed line, best fit of Eq. 1 to experimental I_K. (B) Noisy lines, experimental I_K in 5 μM BrMT at −20, −10, 0, 10, 20, 30, 40, and 50 mV; smooth lines, activation of model BrMT under identical conditions, using a reversal potential of −58.2 mV. (C) Lines are sigmoidicity of fits to I_K from model BrMT. Circles are sigmoidicity from fits of Eq. 1 to experimental I_K. Hollow circles, control condition; filled circles, 5 μM BrMT.

but whatever the complete model entails, to induce cooperative gating, the binding of BrMT must be in some way cooperative. Without cooperative binding, the independent activation of early steps would manifest as a sigmoidicity of $\sigma = 4$ or greater, instead of $\sigma = 2$, which is seen experimentally when BrMT is applied to ShBΔ channels.

The finding that cooperativity was introduced by a ligand was unexpected. Hence, we advise caution in extrapolating conclusions about cooperativity from channels that have been modified by exogenous ligands, mutated, or covalently modified. We find that cooperativity among subunits can be greatly altered by experimental conditions.

We have appreciated the insights of Dr. William Gilly and Dr. Clay Armstrong on this work. We are also indebted to Wayne Kelley in the laboratory of Jonathan Sweedler (University of Illinois Urbana-Champaign, Urbana, IL), who extracted snail glands to isolate the BrMT used in this paper.

This work was partially supported by a grant from the Mathers Foundation.

Lawrence G. Palmer served as editor.

Submitted: 11 January 2006
Accepted: 8 June 2006

REFERENCES

Baker, O.S., H.P. Larsson, L.M. Mannuzzu, and E.Y. Isacoff. 1998. Three transmembrane conformations and sequence-dependent displacement of the S4 domain in shaker K+ channel gating. *Neuron.* 20:1283–1294.

Cherny, V.V., and T.E. DeCoursey. 1999. pH-dependent inhibition of voltage-gated H(+) currents in rat alveolar epithelial cells by Zn(2+) and other divalent cations. *J. Gen. Physiol.* 114:819–838.

Doyle, D.A., J. Morais Cabral, R.A. Pfuetzner, A. Kuo, J.M. Gulbis, S.L. Cohen, B.T. Chait, and R. MacKinnon. 1998. The structure of the potassium channel: molecular basis of K+ conduction and selectivity. *Science.* 280:69–77.

Elinder, F., and P. Arhem. 2003. Metal ion effects on ion channel gating. *Q. Rev. Biophys.* 36:373–427.

Eriksson, M.A., and B. Roux. 2002. Modeling the structure of agitoxin in complex with the Shaker K+ channel: a computational approach based on experimental distance restraints extracted from thermodynamic mutant cycles. *Biophys. J.* 83:2595–2609.

Garcia, M.L., M. Garcia-Calvo, P. Hidalgo, A. Lee, and R. MacKinnon. 1994. Purification and characterization of three inhibitors of voltage-dependent K+ channels from *Leiurus quinquestriatus var. hebraeus* venom. *Biochemistry.* 33:6834–6839.

Gilly, W.F., and C.M. Armstrong. 1982. Divalent cations and the activation kinetics of potassium channels in squid giant axons. *J. Gen. Physiol.* 79:965–996.

Gross, A., and R. MacKinnon. 1996. Agitoxin footprinting the shaker potassium channel pore. *Neuron.* 16:399–406.

Heginbotham, L., and R. MacKinnon. 1992. The aromatic binding site for tetraethylammonium ion on potassium channels. *Neuron.* 8:483–491.

Hidalgo, P., and R. MacKinnon. 1995. Revealing the architecture of a K+ channel pore through mutant cycles with a peptide inhibitor. *Science.* 268:307–310.

Hodgkin, A.L., and A.F. Huxley. 1952. A quantitative description of membrane current and its application to conduction and excitation in nerve. *J. Physiol.* 117:500–544.

Horn, R., S. Ding, and H.J. Gruber. 2000. Immobilizing the moving parts of voltage-gated ion channels. *J. Gen. Physiol.* 116:461–476.

Horrigan, F.T., J. Cui, and R.W. Aldrich. 1999. Allosteric voltage gating of potassium channels I. Mslo ionic currents in the absence of Ca(2+). *J. Gen. Physiol.* 114:277–304.

Hoshi, T., W.N. Zagotta, and R.W. Aldrich. 1990. Biophysical and molecular mechanisms of Shaker potassium channel inactivation. *Science.* 250:533–538.

Kanevsky, M., and R.W. Aldrich. 1999. Determinants of voltage-dependent gating and open-state stability in the S5 segment of Shaker potassium channels. *J. Gen. Physiol.* 114:215–242.

Kelley, W.P., A.M. Wolters, J.T. Sack, R.A. Jockusch, J.C. Jurchen, E.R. Williams, J.V. Sweedler, and W.F. Gilly. 2003. Characterization of a novel gastropod toxin (6-bromo-2-mercaptotryptamine) that inhibits shaker K channel activity. *J. Biol. Chem.* 278: 34934–34942.

Krezel, A.M., C. Kasibhatla, P. Hidalgo, R. MacKinnon, and G. Wagner. 1995. Solution structure of the potassium channel inhibitor agitoxin 2: caliper for probing channel geometry. *Protein Sci.* 4:1478–1489.

Ledwell, J.L., and R.W. Aldrich. 1999. Mutations in the S4 region isolate the final voltage-dependent cooperative step in potassium channel activation. *J. Gen. Physiol.* 113:389–414.

Lenaeus, M.J., M. Vamvouka, P.J. Focia, and A. Gross. 2005. Structural basis of TEA blockade in a model potassium channel. *Nat. Struct. Mol. Biol.* 12:454–459.

Long, S.B., E.B. Campbell, and R. Mackinnon. 2005a. Crystal structure of a mammalian voltage-dependent Shaker family K+ channel. *Science.* 309:897–903.

Long, S.B., E.B. Campbell, and R. Mackinnon. 2005b. Voltage sensor of Kv1.2: structural basis of electromechanical coupling. *Science.* 309:903–908.

Lopez-Barneo, J., T. Hoshi, S.H. Heinemann, and R.W. Aldrich. 1993. Effects of external cations and mutations in the pore region on C-type inactivation of Shaker potassium channels. *Receptors Channels.* 1:61–71.

Lu, Z., A.M. Klem, and Y. Ramu. 2001. Ion conduction pore is conserved among potassium channels. *Nature.* 413:809–813.

MacKinnon, R. 1991. Determination of the subunit stoichiometry of a voltage-activated potassium channel. *Nature.* 350:232–235.

MacKinnon, R., and G. Yellen. 1990. Mutations affecting TEA blockade and ion permeation in voltage-activated K+ channels. *Science.* 250:276–279.

Mannuzzu, L.M., and E.Y. Isacoff. 2000. Independence and cooperativity in rearrangements of a potassium channel voltage sensor revealed by single subunit fluorescence. *J. Gen. Physiol.* 115:257–268.

Murata, Y., H. Iwasaki, M. Sasaki, K. Inaba, and Y. Okamura. 2005. Phosphoinositide phosphatase activity coupled to an intrinsic voltage sensor. *Nature.* 435:1239–1243.

Pathak, M., L. Kurtz, F. Tombola, and E. Isacoff. 2005. The cooperative voltage sensor motion that gates a potassium channel. *J. Gen. Physiol.* 125:57–69.

Ramsey, I.S., M.M. Moran, J.A. Chong, and D.E. Clapham. 2006. A voltage-gated proton-selective channel lacking the pore domain. Nature. 440:1213–1216.

Ranganathan, R., J.H. Lewis, and R. MacKinnon. 1996. Spatial localization of the K+ channel selectivity filter by mutant cycle-based structure analysis. *Neuron.* 16:131–139.

Root, M.J., and R. MacKinnon. 1994. Two identical noninteracting sites in an ion channel revealed by proton transfer. *Science.* 265:1852–1856.

Sack, J.T., R.W. Aldrich, and W.F. Gilly. 2004. A gastropod toxin selectively slows early transitions in the Shaker K channel's activation pathway. *J. Gen. Physiol.* 123:685–696.

Schoppa, N.E., and F.J. Sigworth. 1998a. Activation of shaker potassium channels. I. Characterization of voltage-dependent transitions. *J. Gen. Physiol.* 111:271–294.

Schoppa, N.E., and F.J. Sigworth. 1998b. Activation of Shaker potassium channels. II. Kinetics of the V2 mutant channel. *J. Gen. Physiol.* 111:295–311.

Schoppa, N.E., and F.J. Sigworth. 1998c. Activation of Shaker potassium channels. III. An activation gating model for wild-type and V2 mutant channels. *J. Gen. Physiol.* 111:313–342.

Schumacher, M.A., A.F. Rivard, H.P. Bachinger, and J.P. Adelman. 2001. Structure of the gating domain of a Ca2+-activated K+ channel complexed with Ca2+/calmodulin. *Nature.* 410:1120–1124.

Smith-Maxwell, C.J., J.L. Ledwell, and R.W. Aldrich. 1998a. Role of the S4 in cooperativity of voltage-dependent potassium channel activation. *J. Gen. Physiol.* 111:399–420.

Smith-Maxwell, C.J., J.L. Ledwell, and R.W. Aldrich. 1998b. Uncharged S4 residues and cooperativity in voltage-dependent potassium channel activation. *J. Gen. Physiol.* 111:421–439.

Sokolova, O., L. Kolmakova-Partensky, and N. Grigorieff. 2001. Three-dimensional structure of a voltage-gated potassium channel at 2.5 nm resolution. *Structure.* 9:215–220.

Spires, S., and T. Begenisich. 1994. Modulation of potassium channel gating by external divalent cations. *J. Gen. Physiol.* 104:675–692.

Sun, Y., R. Olson, M. Horning, N. Armstrong, M. Mayer, and E. Gouaux. 2002. Mechanism of glutamate receptor desensitization. *Nature.* 417:245–253.

Terlau, H., J. Ludwig, R. Steffan, O. Pongs, W. Stuhmer, and S.H. Heinemann. 1996. Extracellular Mg2+ regulates activation of rat eag potassium channel. *Pflugers Arch.* 432:301–312.

Yellen, G., D. Sodickson, T.Y. Chen, and M.E. Jurman. 1994. An engineered cysteine in the external mouth of a K+ channel allows inactivation to be modulated by metal binding. *Biophys. J.* 66:1068–1075.

Zagotta, W.N., T. Hoshi, and R.W. Aldrich. 1994a. Shaker potassium channel gating. III: Evaluation of kinetic models for activation. *J. Gen. Physiol.* 103:321–362.

Zagotta, W.N., T. Hoshi, J. Dittman, and R.W. Aldrich. 1994b. Shaker potassium channel gating. II: Transitions in the activation pathway. *J. Gen. Physiol.* 103:279–319.

Zhang, S., S.J. Kehl, and D. Fedida. 2001. Modulation of Kv1.5 potassium channel gating by extracellular zinc. *Biophys. J.* 81:125–136.